LETTERS

Survival times of anomalous melt inclusions from element diffusion in olivine and chromite

C. Spandler[1]†, H. St C. O'Neill[1] & V. S. Kamenetsky[2]

The chemical composition of basaltic magma erupted at the Earth's surface is the end product of a complex series of processes, beginning with partial melting and melt extraction from a mantle source and ending with fractional crystallization and crustal assimilation at lower pressures. It has been proposed that studying inclusions of melt trapped in early crystallizing phenocrysts such as Mg-rich olivine and chromite may help petrologists to see beyond the later-stage processes and back to the origin of the partial melts in the mantle[1,2]. Melt inclusion suites often span a much greater compositional range than associated erupted lavas, and a significant minority of inclusions carry distinct compositions that have been claimed to sample melts from earlier stages of melt production, preserving separate contributions from mantle heterogeneities[1–4]. This hypothesis is underpinned by the assumption that melt inclusions, once trapped, remain chemically isolated from the external magma for all elements except those that are compatible in the host minerals[1,2]. Here we show that the fluxes of rare-earth elements through olivine and chromite by lattice diffusion are sufficiently rapid at magmatic temperatures to re-equilibrate completely the rare-earth-element patterns of trapped melt inclusions in times that are short compared to those estimated for the production and ascent of mantle-derived magma[5,6] or for magma residence in the crust[7]. Phenocryst-hosted melt inclusions with anomalous trace-element signatures must therefore form shortly before magma eruption and cooling. We conclude that the assumption of chemical isolation of incompatible elements in olivine- and chromite-hosted melt inclusions[1,2] is not valid, and we call for re-evaluation of the popular interpretation that anomalous melt inclusions represent preserved samples of unmodified mantle melts.

The ability of a host crystal to isolate and preserve a melt inclusion with a different trace-element signature to the external magma (that is, an anomalous melt inclusion) depends on a negligible flux of the trace elements through the host crystal by lattice diffusion. The process has been modelled mathematically by Qin *et al.*[8], who showed that the isolation of the melt inclusion with respect to a trace element M depends on the diffusion coefficient of M and the partition coefficient between melt and crystal, as well as the dimensions of the inclusion and its host crystal. It has been assumed, often implicitly but sometimes explicitly[1,2,8,9], that the partition coefficients and diffusion coefficients of incompatible trace elements like the rare-earth elements (REEs) in the early crystallizing phases olivine and chromite are so low that isolation is effective: that is, anomalous inclusions are preserved over timescales that are long compared to those expected for magma extraction, ascent and residence in the crust. Although it is true that the concentrations of nearly all the incompatible trace elements in olivine and chromite are very low[10], there are no data on the diffusion coefficients, and thus this most important assumption has never been tested. We have conducted multi-component chemical diffusion experiments on melt-inclusion-hosting olivine and chromite crystals in order to evaluate directly the degree of melt inclusion re-equilibration with an external melt. These experiments also enable us simultaneously to determine the diffusion and partition coefficients for REEs and other elements that are needed for calculating re-equilibration timescales from the mathematical model.

For the olivine experiments, pristine olivine crystals (1–2 mm in size) of composition 89–91% forsterite and containing melt inclusions were hand-picked from a sample of high-Mg mid-ocean-ridge basalt dredged from the southern Mid-Atlantic Ridge (sample AG32-4-68 of ref. 11). The inclusions share similar compositions (Fig. 1) that are typical of primitive high-Mg mid-ocean-ridge basalt liquids[12] (Supplementary Information). Trapping temperatures of 1,230–1,280 °C were recorded for around 50 melt inclusions from homogenization on a heating stage[12]. The host olivines have low REE contents that are consistent with values predicted from relevant olivine/melt partition coefficients[13,14]. A glass of basaltic composition calculated to be in equilibrium with the olivine (90% forsterite) at 1,300 °C was synthesized with ~400 p.p.m. of the REEs Pr, Eu, Tb, Ho and Lu (Supplementary Information). The olivine crystals were combined with the powdered synthetic glass and placed in Re buckets in a gas-mixing furnace and run at 1,300 °C, sufficient to ensure complete remelting of the inclusions, with oxygen fugacity set to $10^{-9.7}$ bar using a flowing CO/CO_2 gas mixture. Run durations were 1, 5 and 25 days, after which the samples were quenched rapidly by dropping into water. Olivine grains were polished to expose the inclusions for analysis of major elements (by energy dispersive spectrometry) and of REEs and selected other trace elements (by laser-ablation inductively coupled plasma mass spectrometry, ICP-MS), with a number of elemental profiles across olivine grains obtained to determine both diffusion coefficients and crystal/melt partition coefficients. The diffusion coefficients are averages from randomly oriented crystallographic sections, suitable for applying to the model of Qin *et al.*[8], which assumes isotropic diffusion. Similar experimental techniques were used for inclusion-hosting chromite grains from the Stillwater Complex[15], except the experimental duration was 7 days at 1,450 °C, to ensure remelting and homogenization of the melt inclusions[15], and to produce easily measurable diffusion profiles. The experimental and analytical techniques are more fully described in the Supplementary Information.

The REE contents in the melt inclusions from the one-day olivine experiment are indistinguishable from the original compositions (Fig. 1a), indicating that diffusive re-equilibration of these inclusions from the synthetic external melt was insignificant. However, sections of the olivine up to 50 μm from the olivine/external melt interface have elevated Lu, Ho and Tb contents. Larger inclusions from the

[1]Research School of Earth Sciences, Australian National University, Canberra 0200, Australia. [2]ARC Centre of Excellence in Ore Deposits and School of Earth Sciences, University of Tasmania, Hobart 7001, Australia. †Present address: Institute of Geological Sciences, University of Bern, Bern 3012, Switzerland.

©2007 Nature Publishing Group

five-day run were also mostly unaffected, but many smaller (<40 μm) inclusions were enriched in Lu, Ho, Tb and Eu (Fig. 1b), and olivine grains had elevated Lu, Ho, Tb and Eu contents to 100 μm from the external melt interface. After 25 days, 21 out of a total of 22 analysed inclusions have modified REE patterns (Fig. 1c). Inclusions with the most extreme REE patterns tend to be small, located within 50 μm of an olivine grain boundary, and are measurably enriched in Pr as well as Lu, Ho, Tb and Eu. They are also depleted in the heavy REEs not added to the external melt (Er, Tm, Yb). Elevated levels of the doped REEs were also found in the olivine crystals, decreasing from the melt/olivine interface towards the interior of the crystal along diffusion profiles (Fig. 2; Supplementary Fig. 1). Similar results were obtained from the chromite experiment. The REE content of chromite has usually been considered insignificant[10], but diffusion of REEs at 1,450 °C is sufficiently rapid that modification of chromite-hosted melt inclusions is observed after only 7 days (Fig. 1d).

All melt inclusions with altered REE patterns show a monotonic increase in the degree of enrichment of the doped REE with atomic number, as do their host olivine or chromite crystals. Lutetium is the most extensively enriched element, followed by Ho, Tb and Eu, with elevated Pr contents only found in inclusions with the most modified REE patterns. Because the external melt was doped with similar contents of the selected REEs (Supplementary Table 1), this fractionation of the REEs in the melt inclusions and olivine cannot be due to physical mixing between the melt inclusions and the external melt, for example along micro-cracks. Furthermore, optical and chemical examination of the olivine and chromite grains indicates that the grains did not undergo dissolution or crystallization during the experiments. The enrichment and fractionation of REEs is attributed solely to diffusion of these elements from the external melt through the olivine and chromite and thence into their melt inclusions. The depletion of Er, Tm and Yb in some of the inclusions (Fig. 1c) is due to diffusion of these elements out of the inclusions, as the external melt is initially devoid of these elements. The general inverse relationship between melt inclusion size and degree of element enrichment (Fig. 1b, c) is expected, because smaller inclusions are more susceptible to diffusive re-equilibration owing to their greater surface area to volume ratio[8,9].

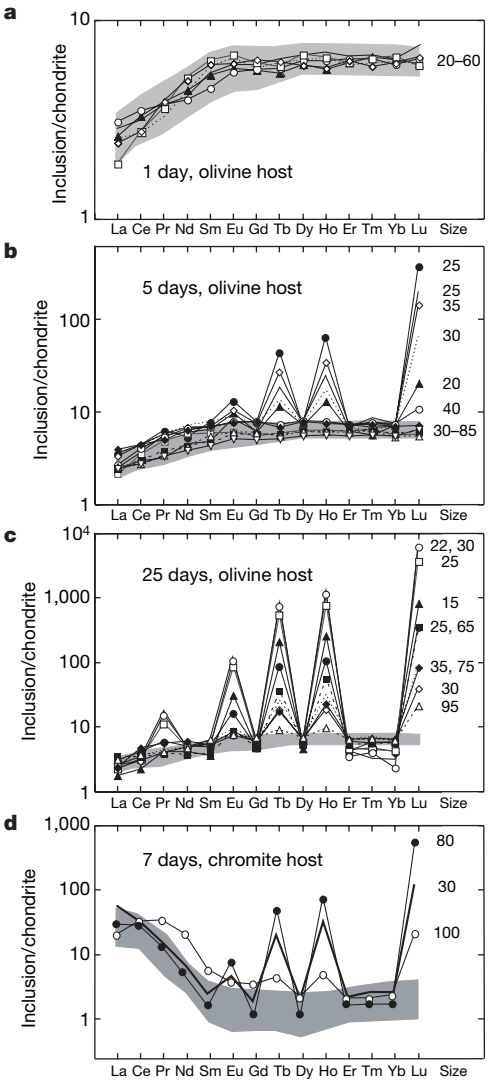

Figure 1 | Chondrite-normalized REE plots of olivine- and chromite-hosted melt inclusions. The grey fields represent the compositional range of normal melt inclusions after homogenization. **a**–**c**, Representative olivine-hosted melt inclusions from the 1-day (**a**), 5-day (**b**) and 25-day (**c**) experiments. **d**, Chromite-hosted melt inclusions from a 7-day experiment. Inclusion size is in μm.

Diffusion coefficients and partition coefficients were obtained by least-squares fitting of the analytical traverses (Fig. 2) (see Supplementary Information). Mean values are given in Table 1 together with observed standard deviations. Our measured diffusion coefficients for Ca and Ni in olivine are in excellent agreement with previous work using quite different experimental approaches[16,17] (see Table 1). A novel feature of our experiments is that the chemical potentials of all relevant major-element oxide components are controlled by the presence of the silicate melt, and moreover are controlled at values appropriate to natural magmas. Previous investigations of diffusion in olivine and other silicates have until recently only controlled oxygen fugacity among chemical potentials, despite the expectation that point-defect concentrations, which determine diffusion rates, depend on other chemical potentials such as silica activity[18,19]. New results on the effect of H_2O on interdiffusion of Mg-Fe^{2+} in olivine demonstrate this clearly[20].

Our reported values of the partition coefficients (K_M) for the REEs between olivine and melt (Table 1) are similar to previously reported values[13,14] (see Supplementary Information). Values of the diffusion coefficients (D_M) of the REEs are identical within experimental error for all REEs in both olivine and chromite, as previously found for garnet, feldspar and apatite, but in contrast to diopside and zircon[21]; the reason for this dichotomy is not known. However, values of the REE diffusion coefficients are two to four orders of magnitude faster

Table 1 | Calculated parameters for olivine and chromite

Element	log D_M ($m^2 s^{-1}$)	$\pm\sigma$	K_M	$\pm\sigma$
Olivine (Mg# ≈ 90; T = 1,300 °C; $f_{O_2} = 10^{-9.7}$ bar)				
Ca	−15.72	0.23	0.015	3×10^{-3}
Ca*	−15.53			
Ca†	−15.39 to −15.25‡			
Ti	−14.99	0.24	0.09	0.03
Ni	−15.20	0.23	20	2
Ni*	−15.21 to −14.82‡			
Pr	−15.17	0.27	17×10^{-5}	3×10^{-5}
Eu	−14.89	0.18	4×10^{-4}	1×10^{-4}
Tb	−14.83	0.14	26×10^{-4}	5×10^{-4}
Ho	−14.86	0.17	7×10^{-3}	1×10^{-3}
Lu	−14.95	0.17	0.033	0.007
Chromite (T = 1,450 °C; $f_{O_2} = 10^{-6.8}$ bar)				
Ni	−14.52	0.57	38.3	15.3
Pr	−14.49	0.47	8×10^{-5}	3×10^{-5}
Eu	−14.61	0.07	20×10^{-5}	5×10^{-5}
Tb	−14.43	0.24	9×10^{-4}	3×10^{-4}
Ho	−14.46	0.26	21×10^{-4}	8×10^{-4}
Lu	−14.50	0.29	76×10^{-4}	26×10^{-4}

Shown are calculated diffusion coefficients (D_M) and partition coefficients (K_M); for each value, uncertainties ($\pm\sigma$) are given in the following column. Note the similarity between Ca and Ni diffusion coefficients calculated from this study and those reported by ref. 16 and ref. 17. f_{O_2}, oxygen fugacity.
* Data from ref. 17 at 1,300 °C and f_{O_2} of $\sim 10^{-9}$ bar.
† Data from ref. 16 at 1,300 °C and f_{O_2} of $\sim 10^{-10}$ bar.
‡ Range is that covered by different crystallographic orientations or varying olivine composition.

©2007 Nature Publishing Group

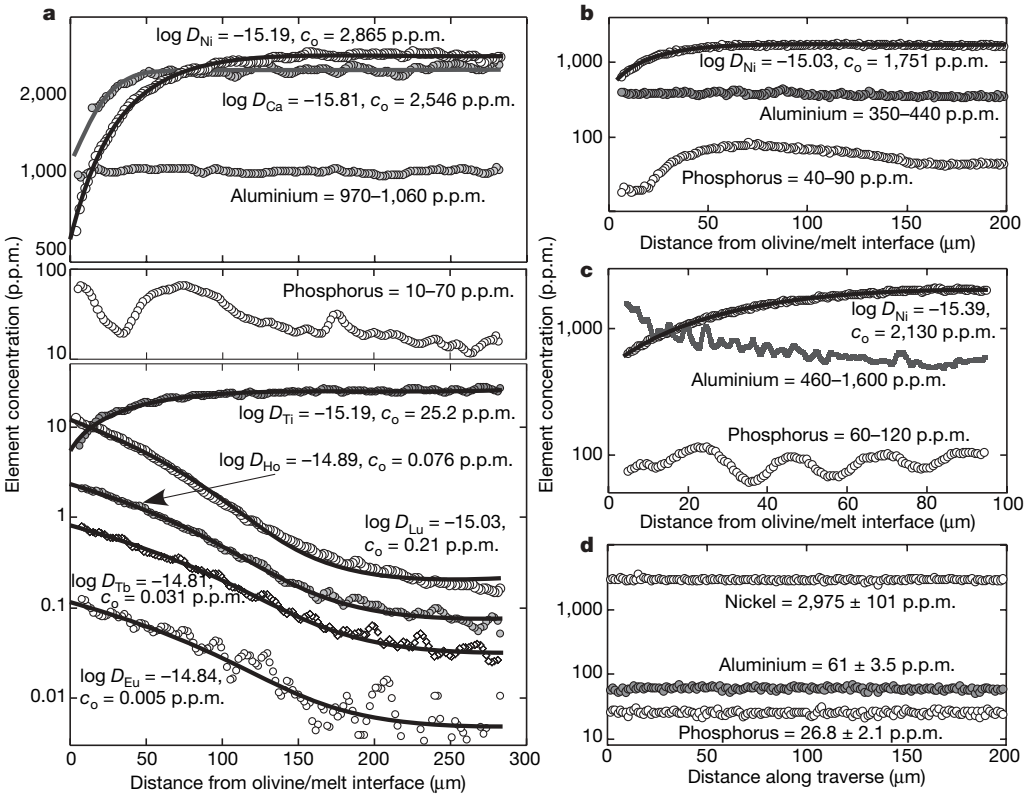

Figure 2 | Measured element diffusion profiles from analytical traverses (obtained by laser ablation ICP-MS) across olivine grains. Solid lines represent the fitted diffusion profiles. **a**, Profiles for Ni, Ca, Al, P, Ti, Lu, Ho, Tb and Eu across olivine from the 25-day experiment. The increased scatter in Eu and Tb values at 150–300 μm from the olivine/melt interface reflect low element concentrations that approach the analytical detection limits. **b**, Profiles for Ni, Al and P across olivine from the 5-day experiment. **c**, Profiles for Ni, Al and P across a second olivine grain from the 25-day experiment. **d**, Profile for Ni, Al and P across the interior of a homogenous olivine from a spinel-lherzolite xenolith (Anakies 9A), for comparison. As P was not present in the melt, any measurable diffusion of P would result in very low levels of this element in the olivine at equilibrium (≤1 p.p.m.). Note the total lack of diffusion of P and the preservation of igneous zoning in the Al and P profiles. Olivines show a variety of original Ni concentrations, but values of D_{Ni} are identical within expected uncertainty. Note the homogeneity of the Anakies 9a olivine compared with the phenocrystal olivines used in the experiments. Details of the data fitting and analysis are presented in the Supplementary Information. The logarithms of diffusion coefficient values (D_M in $m^2 s^{-1}$) and either the original concentration (c_o) or, for non-diffusing elements, concentration ranges, are indicated.

in olivine than in these aforementioned minerals at the same temperature[21], and are remarkably similar to the diffusion coefficients for Mg and Fe^{2+} (ref. 17), the major divalent cations in olivine. The only study addressing the substitution mechanisms of large trivalent cations into olivine found that the substitution of Sc is coupled to vacancies (vac) to maintain charge balance, producing the end-member $(Sc_{2/3}vac_{1/3})_2SiO_4$ (ref. 22). This study found no evidence for Sc coupling with Al (that is, as an $MScAlO_4$ component, where M = Mg or Fe^{2+}). If REEs substitute similarly, then charge balance requires that the diffusion of REEs through the olivine lattice occurs by the mechanism:

$$4/3\,REE^{3+} + M_2SiO_4 = 2\,M^{2+} + (REE_{2/3}vac_{1/3})_2SiO_4$$

The similarity of the observed diffusion coefficients of the REEs to those of Mg and Fe suggest that the latter are the rate-controlling factors for REE diffusion in olivine, which also accounts for the observation that the values of diffusion coefficients for the REEs are independent of atomic number. In contrast to the fast diffusion of REEs, very slow diffusion of Al and P (two elements that may substitute for slow-diffusing Si in the tetrahedral site of olivine) is evident from the absence of any observable diffusion profiles, and from the variety of original magmatic concentrations and zoning patterns that are preserved (Fig. 2). In some crystals (for example, Fig. 2c), Al is heterogeneous on a scale similar to the resolution of the analytical method (~3 μm), suggesting that diffusion rates of Al in olivine are at least three orders of magnitude slower than those of REEs or divalent cations.

It has been assumed that diffusion does not significantly alter the incompatible trace element content of olivine- or chromite-hosted melt inclusions[1,2,8,9] because partition coefficients for these elements in olivine and chromite are low (this work, and refs 10 and 13). However, REE diffusion in these minerals is sufficiently rapid to counter the effects of low partition coefficients, permitting a significant flux of REEs through the olivine and chromite in times that are short compared to those typically proposed for processes of partial melting, magma transport or crustal residence (10 to 10^5 years)[5–7].

We have used our diffusion coefficients and olivine/melt partition coefficients (Table 1) with the mathematical model of Qin *et al.*[8] to calculate timescales of REE re-equilibration between external melt and a 50-μm spherical melt inclusion trapped within a 1-mm olivine grain. Our results show that a melt inclusion will undergo 90% re-equilibration in less than 3 years for the heavy REEs, in around 10 years for the middle REEs and in 20–100 years for the light REEs (Fig. 3). These limiting times may be shortened further in hydrous magmas if the effect of H_2O, not present in our experiments, is included[20]. Recent estimates for the transit times of basalt from its mantle source through the crust range from 30 to $>10^4$ years, from measurements of U-series disequilibria[5] or geophysical modelling of melt extraction processes[6]. Residence times of basaltic magma and associated crystals in the lower crust are also expected to be decades to thousands of years[7]. Our data affirm that even if the shorter timescales for these processes are accepted, the REE patterns of anomalous melt inclusions trapped in olivine phenocrysts in the mantle or lower crust will be extensively modified by lattice diffusion before transport to the Earth's surface. These constraints require olivine-hosted melt

©2007 Nature Publishing Group

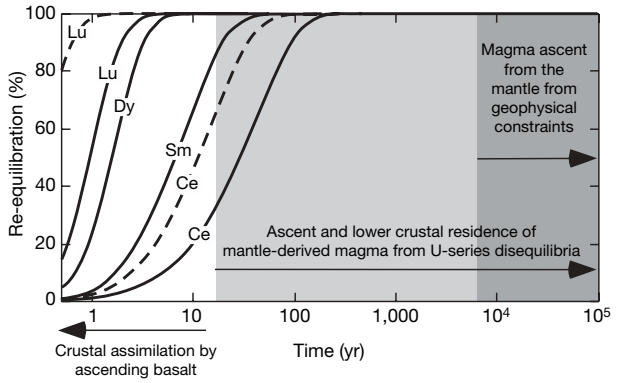

Figure 3 | Modelled re-equilibration times for REEs between a melt inclusion in an olivine grain and an external melt at 1,300 °C. Solid curves, a 50-μm melt inclusion in a 1-mm grain; dashed curve for Lu, a 50-μm melt inclusion in a 0.5-mm grain; dashed curve for Ce, a 30-μm melt inclusion in a 1-mm grain. Re-equilibration was calculated from the equations of ref. 8 using a diffusion coefficient of $10^{-14.9}$ m^2 s^{-1} for all REEs and relevant REE olivine/melt partition coefficients (see Supplementary Fig. 2). Shown for comparison are timescales for basalt transfer from the mantle from U-series disequilibria[5] and from geophysical constraints[6], and residence of basalt and associated crystals in the lower crust[7]—all of which are longer than the time needed for re-equilibration of REE in the melt inclusion. By contrast, timescales of assimilation of crustal material by ascending basalt are relatively short[27].

inclusions with anomalous REE concentrations to be trapped at upper crustal levels shortly (<20 years) before eruption. Melt inclusions trapped in mantle xenoliths from kimberlites, which are transported to the surface in hours to days[23], would be exceptions. This result is consistent with studies that demonstrate some melt inclusion suites to form at relatively low pressures[2,3] or immediately preceding eruption and cooling[24], and we propose that melt inclusion entrapment in phenocrysts is likely to be a late-stage process in general.

Studies of exposed crustal sequences[25,26] and xenocrysts in volcanic rocks[27] indicate that primary mantle melts often experience some degree of reaction and modification during transit through the crust. The fast rates of REE diffusion in olivine and chromite reported here confirm that the isolation of inclusions by these phases may not be sufficient to preserve them against such modification, calling into question the view that anomalous melt inclusions faithfully record signatures of primary melts from the mantle[1–4]. Our results are compatible with alternative proposals that anomalous melt inclusions form either during localized assimilation of crustal rocks—for example, at the margins of a magma chamber or during ascent in a magma conduit[28,29]—or during shallow-level magma mixing[30]. This scenario is consistent with constraints from divalent cation diffusion profiles in olivine xenocrysts, which demonstrate that crustal assimilation by ascending basaltic magmas occurs shortly before eruption (<10 years) (ref. 27). Melt inclusion studies may therefore provide important insights into crustal modification of mantle-derived magmas[28].

Received 20 June 2006; accepted 16 March 2007.

1. Schiano, P. Primitive mantle magmas recorded as silicate melt inclusions in igneous minerals. *Earth-Sci. Rev.* **63,** 121–144 (2003).
2. Sobolev, A. V. Melt inclusions in minerals as a source of principal petrological information. *Petrology* **4,** 209–220 (1996).
3. Sobolev, A. V., Hofmann, A. W. & Nikogosian, I. K. Recycled oceanic crust observed in 'ghost plagioclase' within the source of Mauna Loa lava. *Nature* **404,** 986–990 (2000).
4. Ren, Z.-Y., Ingle, S., Takahashi, E., Hirano, N. & Hirata, T. The chemical structure of the Hawaiian mantle plume. *Nature* **436,** 837–840 (2005).
5. Condomines, M., Gauthier, P.-J. & Sigmarsson, O. Timescales of magma chamber processes and dating of young volcanic rocks. *Rev. Miner. Geochem.* **52,** 125–174 (2003).
6. Faul, U. H. Melt retention and segregation beneath mid-ocean ridges. *Nature* **410,** 920–923 (2001).
7. Reid, M. R. in *Treatise on Geochemistry* Vol. 3, *The Crust* (ed. Rudnick, R. L.) 167–193 (Elsevier Science, Amsterdam, 2003).
8. Qin, Z., Lu, F., Anderson, A. T. Jr., Diffusive reequilibration of melt and fluid inclusions. *Am. Mineral.* **77,** 565–576 (1992).
9. Cottrell, E., Spiegelman, M. & Langmuir, C. H. Consequences of diffusive reequilibration for the interpretation of melt inclusions. *Geochem. Geophys. Geosyst.* **3,** 1026 (2002).
10. Witt-Eickschen, G. & O'Neill, H. St C. The effect of temperature on the equilibrium distribution of trace elements between clinopyroxene, orthopyroxene, olivine and spinel in upper mantle peridotite. *Chem. Geol.* **221,** 65–101 (2005).
11. Le Roex, A. P., Dick, H. J. B., Gulen, L., Reid, A. M. & Erlank, A. J. Local and regional heterogeneity in MORB from the Mid-Atlantic Ridge between 54.5°S and 51°S: Evidence for geochemical enrichment. *Geochim. Cosmochim. Acta* **51,** 541–555 (1987).
12. Kamenetsky, V. Methodology for the study of melt inclusions in Cr-spinel, and implications for parental melts of MORB from FAMOUS area. *Earth Planet. Sci. Lett.* **142,** 479–486 (1996).
13. Kennedy, A. K., Lofgren, G. E. & Wasserburg, G. J. An experimental study of trace element partitioning between olivine, orthopyroxene and melt in chondrules: Equilibrium values and kinetic effects. *Earth Planet. Sci. Lett.* **115,** 177–195 (1993).
14. McKay, G. A. Crystal/liquid partitioning of REE in basaltic systems: Extreme fractionation of REE in olivine. *Geochim. Cosmochim. Acta* **50,** 69–79 (1986).
15. Spandler, C. J., Mavrogenes, J. A. & Arculus, R. J. The origin of chromitites in layered intrusions: Evidence from chromite-hosted melt inclusions from the Stillwater Complex. *Geology* **11,** 893–896 (2005).
16. Jurewicz, A. J. G. & Watson, E. B. Cations in olivine, Part 2: Diffusion in olivine xenocrysts, with applications to petrology and mineral physics. *Contrib. Mineral. Petrol.* **99,** 186–201 (1988).
17. Petry, C., Chakraborty, S. & Palme, H. Experimental determination of Ni diffusion coefficients in olivine and their dependence on temperature, composition, oxygen fugacity, and crystallographic orientation. *Geochim. Cosmochim. Acta* **68,** 4179–4188 (2004).
18. Stocker, R. L. & Smyth, D. M. Effect of enstatite activity and oxygen partial pressure on the point-defect chemistry of olivine. *Phys. Earth Planet. Inter.* **16,** 145–156 (1978).
19. Nakamura, A. & Schmalzried, H. On the nonstoichiometry and point defects of olivine. *Phys. Chem. Miner.* **10,** 27–37 (1983).
20. Hier-Majumder, S., Anderson, I. M. & Kohlstedt, D. L. Influence of protons on Fe-Mg interdiffusion in olivine. *J. Geophys. Res.* **110,** doi:2004JB003292 (2005).
21. Cherniak, D. J. REE diffusion in feldspar. *Chem. Geol.* **193,** 25–41 (2003).
22. Nielsen, R. L., Gallahan, W. E. & Newberger, F. Experimentally determined mineral-melt partition coefficients for Sc, Y, REE for olivine, orthopyroxene, pigeonite, magnetite and ilmenite. *Contrib. Mineral. Petrol.* **110,** 488–499 (1992).
23. Kelley, S. P. & Wartho, J. A. Rapid kimberlite ascent and the significance of Ar-Ar ages in xenolith phlogopites. *Science* **289,** 609–611 (2000).
24. Danyushevsky, L. V., Sokolov, S. & Falloon, T. J. Melt inclusions in olivine phenocrysts: Using diffusive re-equilibration to determine the cooling history of a crystal, with implications for the origin of olivine-phyric volcanic rocks. *J. Petrol.* **43,** 1651–1671 (2002).
25. Bedard, J. H. Oceanic crust as a reactive filter — synkinematic intrusion, hybridization and assimilation in an ophiolitic magma chamber, western Newfoundland. *Geology* **21,** 77–80 (1993).
26. Coogan, L. A. Contaminating the lower crust in the Oman ophiolite. *Geology* **31,** 1065–1068 (2003).
27. Costa, F. & Dungan, M. Short time scales of magmatic assimilation from diffusion modelling of multiple elements in olivine. *Geology* **33,** 837–840 (2005).
28. Danyushevsky, L. V., Leslie, R. A. J., Crawford, A. J. & Durance, P. Melt inclusions in primitive olivine phenocrysts: The role of localized reaction processes in the origin of anomalous compositions. *J. Petrol.* **45,** 2531–2553 (2004).
29. Yaxley, G. M., Kamenetsky, V. S., Kamenetsky, M., Norman, M. D. & Francis, D. Origins of compositional heterogeneity in olivine-hosted melt inclusions from the Baffin Island picrites. *Contrib. Mineral. Petrol.* **148,** 426–442 (2004).
30. Perugini, D., Petrelli, M. & Poli, G. Diffusive fractionation of trace elements by chaotic mixing of magmas. *Earth Planet. Sci. Lett.* **243,** 669–680 (2006).

Supplementary Information is linked to the online version of the paper at www.nature.com/nature.

Acknowledgements M. Shelley, A. Norris and D. Scott are thanked for their help with the laser ablation ICP-MS analyses, electron microprobe analyses, and experimental set-up, respectively. This work was supported by an Australian Research Council Discovery Grant (to H.StC.O'N.).

Author Contributions C.S. prepared and performed the experiments, and H.StC.O'N. fitted the analytical data to obtain diffusion coefficients. C.S. and H.StC.O'N. conducted the microprobe and laser-ablation ICP MS analyses. V.K. characterized and supplied the sample of melt inclusion-bearing olivine phenocrysts. C.S. and H.StC.O'N. co-wrote the paper. All authors discussed the results and commented on the paper.

Author Information Reprints and permissions information is available at www.nature.com/reprints. The authors declare no competing financial interests. Correspondence and requests for materials should be addressed to C.S. (spandler@geo.unibe.ch) or H.StC.O'N. (hugh.oneill@anu.edu.au).

©2007 Nature Publishing Group

doi: 10.1038/nature05759

Survival times of anomalous melt inclusions: Constraints from element diffusion in olivine and chromite

C. Spandler, H. St.C. O'Neill & V. Kamenetsky

Preparation of synthetic external melts

Homogenous synthetic external melts used in the experiments were produced using a sol-gel method[31]. The target compositions of the external melts were designed to be in equilibrium with olivine or chromite at the experimental run conditions. Appropriate amounts of major elements Ca, Al, Fe, Mg, Cr and trace elements Pr, Eu, Tb, Ho, and Lu were combined as nitrate solutions, mixed with tetraethyl orthosilicate ($Si(C_2H_5O)_4$), precipitated, and slowly dried to a gel. The gels were heated in a Pt crucible over a bunsen burner for 30 minutes and then placed in a muffle furnace at 1000 ºC for 2 hours to ensure complete decomposition of the nitrates. The gels were then finely milled and placed in a 1 atmosphere gas-mixing furnace under controlled oxygen fugacity (fO_2) conditions to reduce iron to Fe^{2+}. After 1 hour at 1500 ºC the melted gels were rapidly quenched in water to form glass. To ensure the glass compositions were in equilibrium with olivine or chromite, small amounts of the respective glass compositions were reground and combined with ground olivine or chromite and run at 1300 ºC (for olivine) or 1450 ºC (for chromite) in the 1 atmosphere gas mixing furnace for 1 hour, and then quenched. The composition of these glasses (see below for analytical details) was checked against the starting glasses to evaluate if the starting glasses would be in equilibrium with olivine or chromite at run conditions. Glass compositions were comparable within analytical precision except for the external glass for the olivine

experiments, which was slightly low in Fe. Therefore this glass was reground, combined with additional Fe as Fe_2O_3 and then remelted at 1300 ºC, as described above. Multiple analyses of the glasses for major and trace elements (see below) indicate homogeneity within analytical precision. The final glass compositions are expected to be sufficiently close to being in equilibrium with olivine or chromite at the run conditions that very little dissolution/precipitation will have occurred during the experiments. In any case, such processes will occur, at most, within the first few hours of annealing at run conditions and hence are insignificant over the timescales of the experiments.

Major and trace element analysis of experimental run products

Olivine or chromite grains recovered from experiments were mounted in epoxy and carefully polished to expose melt inclusions. Exposed melt inclusions, minerals and synthetic glasses were analysed for major elements (>0.3 wt%) using an energy-dispersive spectrometer (EDS) equipped, JEOL 6400 scanning electron microscope housed at the Electron Microscope Unit, Australian National University (ANU). Accelerating voltage, beam current and counting time were set at 15 kV, 1 nA and 100 seconds respectively. Element concentrations were standardized against known mineral standards produced by Astimex Scientific Limited. Additional analysis of olivine for major elements and Ca were conducted by wavelength-dispersive spectrometry (WDS) on a Cameca SX 100 electron microprobe at the Research School of Earth Sciences (RSES), ANU. Acceleration voltage was set to 15 kV and a focussed beam of 20 nA current was used. Counting times were 20 seconds on the peak and 20 seconds on the background for each element. In addition, diffusion profiles of Ni, Mn and Ca were

obtained on a number of olivine crystals, since these elements are present in sufficient abundance in natural olivine that reasonably precise measurements may be obtained.

Trace element compositions of minerals, glasses and melt inclusions were determined in-situ by laser-ablation inductively-coupled plasma mass spectrometry (LA ICP-MS) at the RSES, ANU. The method employs an ArF (193 nm) EXCIMER laser and an Agilent 7500 ICP-MS. For melt inclusion analyses, laser repetition rate and the spot size were respectively set to 5-10 Hz and between 19 and 70 μm, depending on inclusion size. Spot sizes of 54 or 70 μm and repetition rates of 5-8 Hz were used for glass and mineral analyses. Counting times were 20 seconds for the background in all analysis and 50 seconds for analysis of minerals and glass. Instrument calibration was against NIST 612 glass using the reference values of ref. 32. The internal standard isotope used to quantify the analyses was ^{43}Ca for the glass, melt inclusions and olivine and ^{27}Al for chromite, based on Ca or Al contents previously measured by EDS or WDS.

Measurement of diffusion profiles

Diffusion coefficients (D_M) in olivine and chromite were obtained from the experiments for a variety of elements from analytical traverses using laser-ablation ICP-MS as follows. The laser was focussed into a 120 x 6 μm rectangular beam oriented parallel to the olivine/melt or chromite/melt interface, and traversed continuously across the mineral at a rate of 5 μm/s, with data for 12 elements recorded every 0.5 s. Some data were also obtained using a conventional 32 μm diameter beam with spots obtained every 50 μm. Samples were orientated with interfaces perpendicular to the plane of the polished section with an optical microscope in reflected light. Raw count data were standardized to NIST 612 glass and converted to element concentrations using ^{29}Si and

^{27}Al as internal standards for olivine and chromite respectively, based on Si and Al contents previously measured by electron microprobe. Additional analytical traverses were conducted on a homogenous olivine grain from an Anakies 9a lherzolite xenolith from Victoria, Australia to confirm the accuracy of the laser traversing technique and the validity of the experimental diffusion profiles. Data from the Anakies 9a traverse is presented in Figure 2d.

Values of D_M were calculated from the analytical profiles assuming a diffusion geometry of one-dimensional trace-element diffusion into a semi-infinite slab with constant composition maintained in the melt at the interface. The solution to the diffusion equation (e.g., ref. 17) under these conditions is:

$$\frac{c(x) - c_o}{c_i - c_o} = 1 - \mathrm{erf}\left(\frac{x}{2(D_M t)^{1/2}}\right)$$

where c(x) is the concentration at distance x, c_i is the concentration at the interface (x=0), c_o is the initial concentration and t the duration of the experiment. Note that this equation may be applied to elements diffusing both into (e.g., REE) and out of (Ti, Ni and Ca in olivine) the crystals (see Fig. 2). The data were fitted directly to the diffusion equation by weighted multiple non-linear least squares, yielding simultaneously values of c_i, c_o, and $(D_M t)^{1/2}$ hence D_M. Values of D_M for each element were calculated from several traverses on olivines from the 25 and 5 day runs and several traverses on chromites from the 7 day run. Graphical examples of the fits are presented in Figure 2 and Supplementary Figure 1. Mean values of D_M are given in Table 1, together with standard deviations.

Calculation of partition coefficients

Values of the olivine/melt and chromite/melt partition coefficients, K_M (Table 1), were calculated from $K_M=c_i/c_{liq}$, where c_{liq} is the concentration in the liquid, and c_i is given above. To our knowledge, we present the first data for REE partitioning between chromite and melt. For both chromite and olivine there is a systematic relationship between REE ionic radii and K_{REE} (Supplementary Fig. 2), with chromite/melt K_{REE} (at 1450 ºC) about half an order of magnitude lower than olivine/melt K_{REE} (at 1300 ºC). Our olivine/melt K_{REE} are similar to previously reported K_{REE} values[13,14]. It is also worth noting that K_{Eu} for olivine and chromite is slightly lower than expected from the trends. This Eu anomaly is attributed to the presence of Eu^{2+} in the melt, due to the relatively low fO_2 conditions of the experiments (Table 1).

Accuracy of the results

There are several lines of evidence that support the accuracy of our measurements of diffusion and partition coefficients:

1) For elements present at sufficient concentrations for reasonably precise electron microprobe analysis, namely Ni, Mn and Ca, diffusion profiles have been determined independently using this method (Supplementary Fig. 1). D_{Ca} calculated from traverses using both electron microprobe and laser ablation ICP-MS agree within error and D_{Ni} calculated from electron microprobe traverses is only slightly slower (logD of 0.3 m^2/s) that D_{Ni} calculated from laser ablation ICP-MS traverses.

2) The concentration profiles in the minerals are fitted by the diffusion equation within analytical uncertainty, both for elements diffusing into and out of the crystals (Fig. 2).
3) The values of D_{Ni} and D_{Ca} in olivine are in excellent agreement with previously published values (Table 1).
4) The values of D_M and K_M for olivine from the 25 day experiment agree with those from the 5 day experiment, although the latter are of course less precise.
5) Calculated K_{REE} in olivine are similar to previously published values (Supplementary Fig. 2).
6) Calculated K_{REE} in olivine and chromite vary systematically with ionic radii (except for a slight Eu anomaly; see Supplementary Fig. 2). On the other hand, in both olivine and chromite, all the REE share the same value of D_{REE} within experimental error, despite the orders-of-magnitude differences in concentrations in the measured diffusion profiles.

Note also that the rapid re-equilibration of the melt inclusions observed directly from our experiments (Fig. 1) is fully supported by the rapid trace-element diffusion through olivine and chromite as evidenced by the diffusion profiles (Fig. 2). The observed diffusion of the undoped heavy REEs (Er, Tm and Yb) out of smaller inclusions (Fig. 2C) also accords with the model. The order-of-magnitude fractionation of the doped REEs (e.g., Pr/Lu) seen in the inclusions and the excellent fit of the analytical profiles to the diffusion equation (Fig. 2; Supplementary Fig. 1) precludes any alternative mechanism to lattice diffusion such as infiltration through cracks or multi-path diffusion involving planar defects.

The method employed here to measure diffusion coefficients is very robust and can give results of the highest accuracy, albeit under a restricted range of conditions. It is

particularly noteworthy that these experiments are the first quantitative diffusion measurements on olivine in which the chemical potentials (that is, activities) of all relevant major-element oxide components are fixed. Previously it has been shown by many studies that fO_2 affects diffusion rates (e.g., ref. 17 and refs. therein), because fO_2 influences the concentration of point defects (refs. 18-19). But these studies also show that activities of MgO, FeO and SiO_2 also affect point defects, hence should also affect diffusion rates. Our study is therefore useful in showing that, at least for Ni and Ca, the diffusion coefficients obtained previously in experiments in which fO_2 was the only chemical potential to be controlled are indeed applicable to natural environments.

The long diffusion profiles and the presence of silicate melt to effect annealing minimise inaccuracies from surface roughness and microcracking, which may severely affect results from conventional diffusion couples. On the other hand, it is only possible to study elements covering a limited range of diffusion rates in any one experiment, as the duration of the experiment must be selected to give a diffusion profile of suitable dimensions (optimally a profile should cover >100 μm).

Supplementary references

31. Luth, W. C. & Ingamells, O. Gel preparation of starting materials for hydrothermal experimentation. *Am. Mineral.* **50,** 255-258 (1965).

32. Pearce, N. J. G., Perkins, W. T., Westgate, J. A., Gorton, M. J., Jackson, S. E., Neal, C. R. & Chenery, S. P. A compilation of new and published major and trace element data for NIST SRM 610 and NIST SRM 612 glass reference materials. *Geostand. News.* **21,** 115-144 (1997).

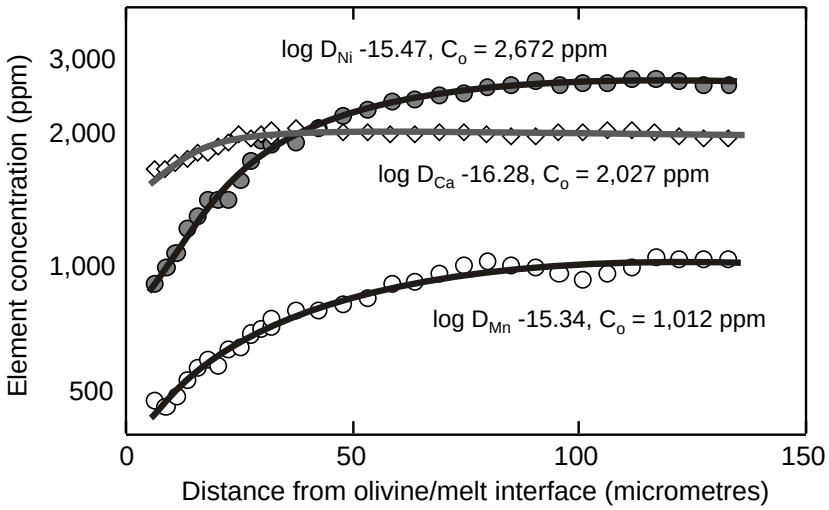

Supplementary Figure 1. Measured and fitted diffusion profiles for Ni, Ca and Mn from electron microprobe analytical traverses across olivine grain towards the olivine/melt interface. The olivine grain is from the 25-day experiment. The logarithms of diffusion coefficient values (D_M in m^2/s) and original concentration (C_O) are indicated.

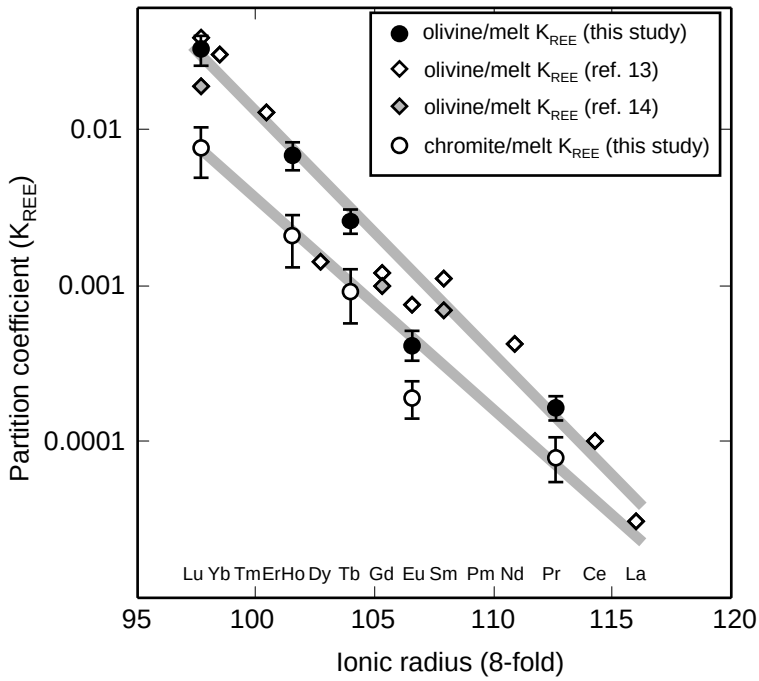

Supplementary Figure 2. Plot of olivine/melt and chromite/melt partition coefficients obtained from this study versus REE ionic radius. Ranges of one standard deviation are shown as the error bars. Also shown for comparison are relevant olivine/melt partition coefficients of ref. 13 and ref. 14. Grey lines are best-fit trends to the data. Note that Eu falls off the trend, indicating some Eu may be present as Eu^{2+} in our experiments.

Supplementary Table 1. Major and trace element compositions of the synthetic external melt used for the olivine experiments (1), homogenised olivine-hosted melt inclusions (2-3) and selected melt inclusions from diffusion experiments (4-10).

Label	1	2	3	4	5	6	7	8	9	10
Exp. duration		10 hours	10 hours	1 day	5 days	5 days	25 days	25 days	25 days	25 days
Size (µm)		55	30	25	25	45	35	25	95	35
Major element oxides (wt%)										
SiO_2	53.46	47.85	48.54	48.07	47.98	47.57	47.92	48.68	48.39	47.61
TiO_2	-	0.63	0.45	0.53	0.67	0.61	0.64	0.38	0.67	0.68
Al_2O_3	14.88	15.31	15.05	14.65	14.94	15.11	15.62	17.91	15.98	15.65
FeO	5.81	7.90	8.21	8.63	8.39	8.62	8.36	6.08	7.67	8.14
MgO	15.29	13.43	13.37	13.39	13.23	13.29	12.97	13.73	12.87	13.06
CaO	10.05	12.43	12.48	11.65	11.10	11.82	11.13	11.17	11.65	11.25
Na_2O	-	1.34	1.51	1.68	1.89	1.58	1.61	1.59	1.75	1.52
K_2O	-	bd	bd	bd	bd	0.04	bd	bd	bd	bd
Total	99.49	99.12	99.87	98.60	98.20	98.93	98.25	99.54	98.97	97.91
Trace elements (ppm)										
La	0.9*	1.08	0.72	0.70	1.15	0.89	1.01	0.83	1.18	1.04
Ce	nd	2.93	2.46	2.65	3.89	2.93	3.40	3.10	3.56	3.43
Pr	381	0.40	0.43	0.50	1.04	0.52	0.60	1.56	0.57	0.61
Nd	nd	2.56	2.97	3.69	5.18	3.11	3.41	3.53	3.44	3.54
Sm	nd	1.06	1.17	1.46	1.90	1.10	1.39	1.26	1.48	1.43
Eu	393	0.45	0.47	0.59	1.12	0.50	0.98	7.51	0.67	0.84
Gd	10*	1.67	1.58	1.89	1.77	1.77	1.92	1.83	2.15	1.84
Tb	346	0.32	0.32	0.34	1.86	0.33	2.86	32.6	0.53	1.53
Dy	nd	2.26	2.34	2.57	2.48	2.34	2.49	2.17	2.65	2.63
Ho	361	0.50	0.53	0.56	3.15	0.52	5.89	66.4	0.84	2.75
Er	nd	1.52	1.49	1.54	1.60	1.59	1.59	1.16	1.61	1.65
Tm	nd	0.23	0.22	0.27	0.24	0.22	0.22	0.16	0.24	0.26
Yb	0.04*	1.59	1.54	1.64	1.71	1.45	1.51	1.07	1.56	1.59
Lu	383	0.23	0.24	0.23	6.30	0.24	10.24	141	0.82	3.69
Percent re-equilibration										
Pr	-	-	-	<0.03	0.07	<0.03	<0.03	0.26	<0.03	<0.03
Eu	-	-	-	<0.03	0.13	<0.03	0.11	1.79	<0.03	0.08
Tb	-	-	-	<0.03	0.44	<0.03	0.72	9.30	0.04	0.34
Ho	-	-	-	<0.03	0.72	<0.03	1.48	18.3	0.07	0.60
Lu	-	-	-	<0.03	1.58	<0.03	2.61	36.8	0.15	0.90

Notes: * La, Gd and Yb concentrations in the synthetic external melt are presumably from impurities in starting chemicals.
nd = not detected, bd = below detection limit.

Supplementary Table 1. Major and trace element compositions of the synthetic external melt used for the olivine experiments (1), homogenised olivine-hosted melt inclusions (2-3) and selected melt inclusions from diffusion experiments (4-10).

Label	1	2	3	4	5	6	7	8	9	10
Exp. duration		10 hours	10 hours	1 day	5 days	5 days	25 days	25 days	25 days	25 days
Size (µm)		55	30	25	25	45	35	25	95	35
Major element oxides (wt%)										
SiO_2	53.46	47.85	48.54	48.07	47.98	47.57	47.92	48.68	48.39	47.61
TiO_2	-	0.63	0.45	0.53	0.67	0.61	0.64	0.38	0.67	0.68
Al_2O_3	14.88	15.31	15.05	14.65	14.94	15.11	15.62	17.91	15.98	15.65
FeO	5.81	7.90	8.21	8.63	8.39	8.62	8.36	6.08	7.67	8.14
MgO	15.29	13.43	13.37	13.39	13.23	13.29	12.97	13.73	12.87	13.06
CaO	10.05	12.43	12.48	11.65	11.10	11.82	11.13	11.17	11.65	11.25
Na_2O	-	1.34	1.51	1.68	1.89	1.58	1.61	1.59	1.75	1.52
K_2O	-	bd	bd	bd	bd	0.04	bd	bd	bd	bd
Total	99.49	99.12	99.87	98.60	98.20	98.93	98.25	99.54	98.97	97.91
Trace elements (ppm)										
La	0.9*	1.08	0.72	0.70	1.15	0.89	1.01	0.83	1.18	1.04
Ce	nd	2.93	2.46	2.65	3.89	2.93	3.40	3.10	3.56	3.43
Pr	381	0.40	0.43	0.50	1.04	0.52	0.60	1.56	0.57	0.61
Nd	nd	2.56	2.97	3.69	5.18	3.11	3.41	3.53	3.44	3.54
Sm	nd	1.06	1.17	1.46	1.90	1.10	1.39	1.26	1.48	1.43
Eu	393	0.45	0.47	0.59	1.12	0.50	0.98	7.51	0.67	0.84
Gd	10*	1.67	1.58	1.89	1.77	1.77	1.92	1.83	2.15	1.84
Tb	346	0.32	0.32	0.34	1.86	0.33	2.86	32.6	0.53	1.53
Dy	nd	2.26	2.34	2.57	2.48	2.34	2.49	2.17	2.65	2.63
Ho	361	0.50	0.53	0.56	3.15	0.52	5.89	66.4	0.84	2.75
Er	nd	1.52	1.49	1.54	1.60	1.59	1.59	1.16	1.61	1.65
Tm	nd	0.23	0.22	0.27	0.24	0.22	0.22	0.16	0.24	0.26
Yb	0.04*	1.59	1.54	1.64	1.71	1.45	1.51	1.07	1.56	1.59
Lu	383	0.23	0.24	0.23	6.30	0.24	10.24	141	0.82	3.69
Percent re-equilibration										
Pr	-	-	-	<0.03	0.07	<0.03	<0.03	0.26	<0.03	<0.03
Eu	-	-	-	<0.03	0.13	<0.03	0.11	1.79	<0.03	0.08
Tb	-	-	-	<0.03	0.44	<0.03	0.72	9.30	0.04	0.34
Ho	-	-	-	<0.03	0.72	<0.03	1.48	18.3	0.07	0.60
Lu	-	-	-	<0.03	1.58	<0.03	2.61	36.8	0.15	0.90

Notes: * La, Gd and Yb concentrations in the synthetic external melt are presumably from impurities in starting chemicals. nd = not detected, bd = below detection limit.